

AFRL-VS-HA-TR-98-0080

**CONTINUED IMPROVEMENTS TO THE PRISM
AND PIM IONOSPHERIC MODELS**

**Robert E. Daniell, Jr.
Lincoln D. Brown**

**Computational Physics, Inc.
240 Bear Hill Road, Suite 202A
Waltham, MA 02451**

22 June 1998

Scientific Report No. 2

Approved for public release; distribution unlimited



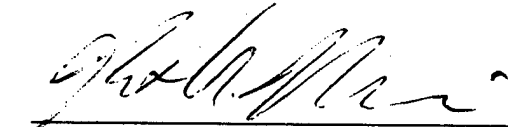
**AIR FORCE RESEARCH LABORATORY
Space Vehicles Directorate
29 Randolph Road
AIR FORCE MATERIEL COMMAND
HANSCOM AFB, MA 01731-3010**

19990923 076

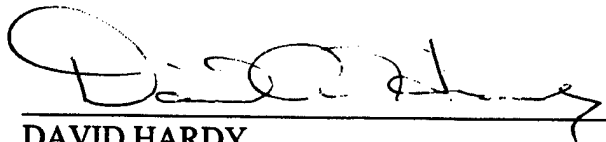
This technical report has been reviewed and is approved for publication.



PETER J. SULTAN
Contract Manager



ROBERT MORRIS
Branch Chief



DAVID HARDY
Division Director

This report has been reviewed by the ESC Public Affairs Office (PA) and is releasable to the National Technical Information Service (NTIS).

Qualified requestors may obtain additional copies from the Defense Technical Information Center (DTIC). All others should apply to the National Technical Information Service (NTIS).

If you change your address, wish to be removed from this mailing list, or your organization no longer employs the addressee, please notify AFRL/VSRTM, 29 Randolph Road, Hanscom AFB, MA 01731-1010. This will assist us in maintaining a current mailing list.

Do not return copies of this report unless contractual obligations or notices on a specific document require that it be returned.

REPORT DOCUMENTATION PAGE			Form Approved OMB No. 0704-0188	
Public reporting burden for this collection of information is estimated to average 1 hour per response, including the time for reviewing instructions, searching existing data sources, gathering and maintaining the data needed, and completing and reviewing the collection of information. Send comments regarding this burden estimate or any other aspect of this collection of information, including suggestions for reducing this burden, to Washington Headquarters Services, Directorate for Information Operations and Reports, 1215 Jefferson Davis Highway, Suite 1204, Arlington, VA 22202-4302, and to the Office of Management and Budget, Paperwork Reduction Project (0704-0188), Washington, DC 20503.				
1. AGENCY USE ONLY (Leave blank)	2. REPORT DATE 22 June 1998	3. REPORT TYPE AND DATES COVERED Scientific No. 2 (11 Aug 96 – 10 Aug 97)		
4. TITLE AND SUBTITLE Continued Improvements to the PRISM and PIM Ionospheric Models		5. FUNDING NUMBERS PE 63790F PR 4026 TA GL WU MD		
6. AUTHOR(S) Robert E. Daniell, Jr., and Lincoln D. Brown		Contract F19628-95-C-0079		
7. PERFORMING ORGANIZATION NAME(S) AND ADDRESS(ES) Computational Physics, Inc. Suite 202A 240 Bear Hill Road Waltham, MA 02154		8. PERFORMING ORGANIZATION REPORT NUMBER		
9. SPONSORING / MONITORING AGENCY NAME(S) AND ADDRESS(ES) Air Force Research Laboratory 29 Randolph Road Hanscom AFB, MA 01731-3010 Contract Manager: Peter Sultan/VSBP		10. SPONSORING / MONITORING AGENCY REPORT NUMBER AFRL-VS-HA-TR-98-0080		
11. SUPPLEMENTARY NOTES				
12A. DISTRIBUTION / AVAILABILITY STATEMENT APPROVED FOR PUBLIC RELEASE; DISTRIBUTION UNLIMITED			12b. DISTRIBUTION CODE	
13. ABSTRACT (Maximum 200 words) This report describes the modifications and updates that have been made to the Parameterized Real-time Ionospheric Specification Model (PRISM) that is operational at the 55 th Space Weather Squadron (55 SWXS). It also describes the implications of work carried out under a separate contract for the design and development of a new version of PRISM (to be known as PRISM 2) that is to include the plasmasphere, improved theoretical climatology, and an improved data assimilation algorithm.				
14. SUBJECT TERMS ionosphere, space environment, data assimilation, space weather, ionospheric specification			15. NUMBER OF PAGES	
			16. PRICE CODE	
17. SECURITY CLASSIFICATION OF REPORT Unclassified	18. SECURITY CLASSIFICATION OF THIS PAGE Unclassified	19. SECURITY CLASSIFICATION OF ABSTRACT Unclassified	20. LIMITATION OF ABSTRACT SAR	

Table of Contents

Executive Summary	v
1. Introduction	1
2. The High Altitude Extension to PRISM and PIM	1
3. References	3
Appendix A. PRISM Updates	5
Appendix B. Derivation of the Multi-ion Ambipolar Diffusion Equation for GTIM	19

This page is intentionally blank.

Executive Summary

Due to a lower level of funding than originally anticipated, the emphasis of the second year of this contract has been on supporting the existing version of the Parameterized Real-time Ionospheric Specification Model (PRISM) by providing updates and bug fixes as problems were uncovered by Computational Physics, Inc. (CPI) and by other users of PRISM. Nevertheless, work aimed at the development of PRISM 2 has continued at a low level. A working, multi-ion version of GTIM being necessary both to this effort and to a separate development effort funded under a separate contract (F19628-96-C-0041), development of the said version of GTIM took place under the other contract. However, the implications of this work for PRISM 2 are described in this report along with a summary of the updates and changes made to the current operational version of PRISM.

1. INTRODUCTION

The primary objective of this contract is the improvement of the Parameterized Real-time Ionospheric Specification Model (PRISM). This objective has several components including (1) improvement of PRISM's base climatology, i.e., the Parameterized Ionospheric Model (PIM), (2) extending PRISM (and PIM) to include the plasmasphere, and (3) improving PRISM's data assimilation algorithm. The first two objectives will be accomplished by parameterizing a single, global, physics-based, multi-ion ionospheric model (AFRL's Global Theoretical Ionospheric Model, GTIM) instead of the separate regional ionospheric models used in the original PRISM development effort. The new version of PRISM will be called PRISM 2.0 and will incorporate other improvements as well. A secondary objective of this contract is the continued support of PRISM 1.6, which is the operational version at the 50th Weather Squadron at Falcon AFB, (2) the development of PRISM applications such as three dimensional ray tracing software, and (3) the development of visualization software for use with PRISM output.

The emphasis of the second year of this contract was on providing support for the current version of PRISM while preparations for the production of PRISM 2 continued at a lower level than during the first year. This was due in part to a difficulty that we encountered with the light ion version of GTIM. This difficulty is described in Section 2. Modifications to the current version of PRISM to correct problems that have been uncovered by various PRISM users are described in Appendix A.

The content of this report reflects the state of the effort as of August 1997. A number of things have changed since then, and the reader is urged to consult later reports in this series for more current descriptions of PRISM development.

2. THE HIGH ALTITUDE EXTENSION TO PRISM AND PIM

The Parameterized Real-time Ionospheric Specification Model (PRISM) has been described by *Daniell et al.* [1990] and *Anderson* [1993]. The climatological model on which PRISM is based, known as PIM, has been described by *Daniell et al.* [1995]. The validation of an early version of PRISM was described by *Daniell et al.* [1993]. Some of the design considerations for the development of PRISM 2 were described in *Daniell et al.* [1998].

One of the important innovations to be used in this development was a new version of the AFRL Global Theoretical Ionospheric Model (GTIM) that included the light ions H^+ and He^+ , allowing the modeling of the plasmasphere. In the process of implementing GTIM on our in-house computers to make production runs for PRISM 2 and for another contract, we found the code to be subject to numerical instabilities. In the process of diagnosing the source of these instabilities, we realized that there was a problem with the use of this approach for the plasmaspheric field lines ($L > ?$).

GTIM was developed from the older code, LOWLAT, which was developed by *Anderson* [1973] to solve for O^+ along flux tubes. (O^+ is the dominant ion in the F region of the

ionosphere, which is the main part of the ionosphere.) The method is based on the concept of ambipolar diffusion, in which the inertial terms of the momentum equation are neglected and charge neutrality ($n_e = n_{O^+}$) and parallel flux balance ($n_e \mathbf{v}_e \cdot \hat{\mathbf{b}} = n_{O^+} \mathbf{v}_{O^+} \cdot \hat{\mathbf{b}}$) are enforced. The continuity equation for O^+ is

$$\frac{\partial n_{O^+}}{\partial t} + \hat{\mathbf{b}} \cdot \nabla (n_{O^+} \mathbf{v}_{O^+}) + (n_{O^+} \mathbf{v}_{O^+}) \cdot \nabla \hat{\mathbf{b}} + \nabla \cdot \left(\frac{\mathbf{E} \times \mathbf{B}}{B^2} \right) = P_{O^+} - L_{O^+} \quad (1)$$

The O^+ flux may be obtained from the electron and O^+ momentum equations by using the flux balance condition, neglecting inertial terms:

$$n_{O^+} \mathbf{v}_{O^+} \cdot \hat{\mathbf{b}} = \frac{1}{\nu_{O^+}} \left\{ n_{O^+} \mathbf{g} \cdot \hat{\mathbf{b}} - \frac{k}{m_{O^+}} \hat{\mathbf{b}} \cdot \nabla [n_{O^+} (T_{O^+} + T_e)] \right\} + n_{O^+} \mathbf{v}_n \cdot \hat{\mathbf{b}} \quad (2)$$

Upon substitution of Eq. (2) into Eq. (1), one obtains a linear diffusion equation which in LOWLAT is solved using the Crank-Nicholson method. The chief problem with this approach is that the collision frequency ν_{O^+} becomes very small at high altitudes (where O^+ may not be the dominant ion) leading to numerical instabilities. This was handled in LOWLAT by adding to the actual collision term a constant so that the collision frequency cannot fall below the constant value.

When one extends the preceding equations to include additional ions, the resulting coupled diffusion equations become nonlinear. The full derivation of the multi-ion ambipolar diffusion equations is given in Appendix B. The impact of this non-linearity on the solution method used in GTIM had not been properly assessed before CPI was given access to the code. The original solution method was simply to apply the linear solver to the three separate ions without taking into account the additional terms that appear in the multi-ion equations, but vanish when only one ion is present. Working primarily under the contract F19628-96-C-0041 (for which a working, multi-ion version of GTIM was a prerequisite), we modified the code to be consistent with the proper multi-ion equations. In that case, it does not appear that the collision frequencies need to be modified to avoid numerical instabilities, a definite advantage of this approach.

As of August 1997, we were still studying the implications of this situation and the behavior of the code. It was not clear that the solutions being obtained were, in fact, correct. Although the O^+ densities appeared to be consistent with observations and other models, the H^+ and He^+ densities were behaving properly. We will report on the results of our investigations and the resolution of the problem in future reports.

3. REFERENCES

- Anderson, D. N., A theoretical study of the ionospheric *F* region equatorial anomaly—Theory, *Planet. Space Sci.*, **21**, 409-419, 1973.
- Anderson, D. N., The development of global, semi-empirical ionospheric specification models, in *Proceedings of the Ionospheric Effects Symposium*, J. M. Goodman, ed., pp. 353-363, 4-6 May 1993.
- Brace, L. H., and R. F. Theis, Global empirical models of ionospheric electron temperature in the upper *F*-region and plasmasphere based on in situ measurements from the Atmospheric Explorer-C, ISIS 1, and ISIS 2 satellites, *J. Atmos. Terr. Phys.*, **43**, 1317, 1981.
- Daniell, R. E., D. T. Decker, D. N. Anderson, J. R. Jasperse, J. J. Sojka, and R. W. Schunk, A Global Ionospheric Conductivity and Electron Density (ICED) Model, in *Proceedings of the Ionospheric Effects Symposium*, J. M. Goodman, ed., 1-3 May 1990.
- Daniell, R. E., W. G. Whartenby, and D. N. Anderson, PRISM Validation, in *Proceedings of the Ionospheric Effects Symposium*, J. M. Goodman, ed., pp. 364-368, 4-6 May 1993.
- Daniell, R. E., L. D. Brown, D. N. Anderson, M. W. Fox, P. H. Doherty, D. T. Decker, J. J. Sojka, and R. W. Schunk, Parameterized ionospheric model: A global ionospheric parameterization based on first principles models, *Radio Sci.*, **30**, 1499-1510, 1995.
- Daniell, R. E., L. D. Brown, and R. P. Barnes, Modifications and Improvements to the PRISM and PIM Ionospheric Models, AFRL-VS-HA-TR-98-0079, June 1998.
- Decker, D. T., C. E. Valladares, R. Sheehan, Su. Basu, D. N. Anderson, and R. A. Heelis, Modeling daytime *F* layer patches over Sondrestrom, *Radio Sci.*, **29**, 249-268, 1994.
- Fejer, B. G., E. R. de Paula, R. A. Heelis, and W. B. Hanson, Global equatorial ionospheric vertical plasma drifts measured by the AE-E satellite, *J. Geophys. Res.*, **100**, 5769-5776, 1995.
- Hardy, D. A., M. S. Gussenhoven, R. Raistrick, and W. J. McNeil, Statistical and functional representations of the pattern of auroral energy flux, number flux, and conductivity, *J. Geophys. Res.*, **92**, 12,275-12,294, 1987.
- Hardy, D. A., W. McNeil, M. S. Gussenhoven, and D. Brautigam, A statistical model of auroral ion precipitation, 2, Functional representation of the average patterns, *J. Geophys. Res.*, **96**, 5539-5547, 1991.
- Heppner, J. P., and N. C. Maynard, Empirical high-latitude electric field models, *J. Geophys. Res.*, **92**, 4467-4489, 1987.

Rich, F. J., and N. C. Maynard, Consequences of using simple analytical functions for the high-latitude convection electric field, *J. Geophys. Res.*, *94*, 3687-3701, 1989.

Strickland, D. J., J. S. Evans, and L. J. Paxton, Satellite remote sensing of thermospheric O/N₂ and solar EUV, 1. Theory, *J. Geophys. Res.*, *100*, 12,217-12,226, 1995.

Appendix A

PRISM Updates

Contents: PRISM changes memoranda for the period 12 August 1995 through 19 August 1996.

Memo date	PRISM version	Page
1996 September 30	1.6b to 1.7	6
1996 November 7	1.7 to 1.7a	11
1997 February 14	1.7a to 1.7b	17

M·E·M·O·R·A·N·D·U·M

DATE: 30-September-1996

TO: Rob Daniell

FROM: Lincoln Brown

RE: Changes to PRISM 1.6b for PRISM 1.7

The changes to PRISM 1.6b for PRISM 1.7 focus on replacing the LLF coefficient set again, on improving the handling of collocated data in the real-time adjustment, and on improving the merging of the parameterized model density profiles. The changes are summarized as follows:

- I. **BUG FIX:** The LLF parameterized model coefficient set has been replaced again. Because of a bug in the processing of the LOWLAT output, the magnetic latitude grid in the PRISM 1.6b LLF coefficient files was defined to start at -33°N instead of the correct value of -34°N. This resulted in an erroneous northward 1° magnetic latitude shift in the O⁺ densities from the LLF parameterized model. The LLF coefficient files have been regenerated with the correct starting value for the magnetic latitude grid. Note that this fix requires no change to the PRISM source code.
- II. **BUG FIX:** The conversion of UT from hours to HHMM in routine PARAM for the URSI f_oF₂ model has been corrected. Previously, the conversion of UT from decimal hours to HHMM resulted in truncation of the minutes to zero, e.g. a UT of 1.5 hours was erroneously converted to 0100. The conversion has been modified so that the minutes are not truncated to zero, e.g. a UT of 1.5 hours is correctly converted to 0130.
- III. Based on work done by Pat Doherty, we now recommend that a 27-day running mean of F_{10.7} be used instead of a daily value. Pat found that a mean F_{10.7} correlates much better with the ionosphere than a daily value, either because the solar EUV has less day-to-day variability than F_{10.7} or because the day-to-day variability in solar EUV is uncorrelated with the day-to-day variability in F_{10.7}. The same applies to Sunspot Number (use a 27-day running mean instead of a daily value), although we recommend using F_{10.7} instead of Sunspot Number as the solar activity index.
- IV. Multiple data points critically close to an output grid point are now handled correctly in the real-time adjustment. Previously, if one or more data points was within the critical distance of an output grid point, then the correction returned by the real-time adjustment was the correction from the last data point within the critical distance. Now, if one or more data points are within the critical distance of an output grid point, then the correction returned from the real-time adjustment is the average of corrections from those data points.
- V. The top-level parameterized model routine PARAM has undergone substantial changes. The original motivation was a report from Jim Secan at Northwest Research Associates illustrating a discontinuity in PRISM 1.6b TEC at the latitude transition region between the

mid-latitude and high-latitude parameterized models. A closer examination of routine PARAM has yielded the following improvements:

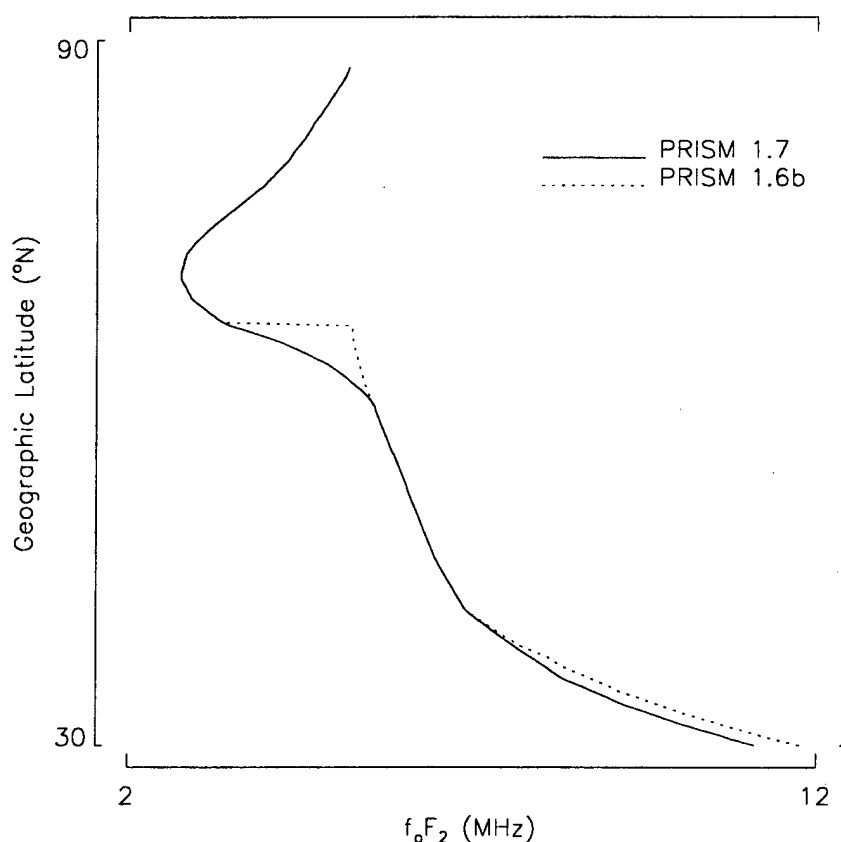
- A. It has been completely rewritten for optimization and readability. The number of routine calls has been reduced.
 - B. The transition between the mid-latitude and high-latitude parameterized models is smoother. Previously, in the mid/high-latitude transition region, the mid-latitude peak density and height were used to merge the mid-latitude and high-latitude density profiles, resulting in a discontinuity in density at the boundary between the high-latitude region and the mid/high-latitude transition region. Now, weighted averages of mid-latitude and high-latitude peak densities and heights are used in the merging, resulting in a smoother transition.
 - C. The transition between the low-latitude and mid-latitude parameterized models is smoother. Previously, a weighted average of low-latitude and mid-latitude critical frequencies was used to calculate the peak density for the merging of the low-latitude and mid-latitude density profiles. Now, the peak density used in the merging is calculated from a weighted average of low-latitude and mid-latitude peak densities. This is consistent with the profile merging process, and results in a smoother transition between the low-latitude and mid-latitude parameterized models.
- VI. The mid-level parameterized model routines LOW_PARAM, MID_PARAM, and USUMODEL have been rewritten to accommodate changes in the top-level parameterized model routine PARAM, to provide small performance gains by reducing routine calls and eliminating unnecessary calculations, and to improve readability.
- VII. The low-level parameterized USU model routines RECON, FOUR_COEFF, and FULL_DATA have been modified to accommodate changes to the mid-level parameterized model routine USUMODEL.
- VIII. Several routines in module ENVIRON.FOR have been replaced for compatibility with PIM.
- IX. Several routines have been modified to accommodate the new version of routine SOLDEC.
- X. Several minor changes have been made for compatibility with Microsoft FORTRAN. They do not impact the results.
- The table below describes the changes that I made to PRISM 1.6b to produce PRISM 1.7.

Module	Program Unit	Description of Changes
ADJ_FNH.FOR	Subroutine GET_FOS	Removed argument ERR from the call to INFLECTION since it is no longer used by that routine. Removed local variable ERR since it is no longer used.
	Subroutine INFLECTION	Removed input argument ERR since it is not used. Changed declaration of local variable TEST from LOGICAL*1 to LOGICAL.
	Subroutine GET_FOE	Removed since it is no longer used.
ENVIRON.FOR	Subroutine SOLZA	Removed since it has been replaced by routine SOLSZA.
	Subroutine SSOLPT	Removed since it has been replaced by routine SOLSUB.
	Function SOLDEC	Replaced by routine of the same name.
	Function SOLANG	New routine.
	Subroutine SOLSUB	New routine.
	Function SOLSZA	New routine.
FMODEL.FOR	Subroutine FMODEL	Removed argument HBOT from call to PARAM since it is not used by that routine. Removed last argument in call to PARAM since it is no longer used by that routine. Removed local variable HBOT since it is no longer used.
GETDAT.FOR	Subroutine GETDAT	Removed argument ESWITCH from call to MODEL_FLAGS since it is no longer used.
	Subroutine MODEL_FLAGS	Removed assignment of input argument ESW. Removed input argument ESW since it is no longer used.
	Subroutine PREC_DATA	Changed declaration of local variable TEST from LOGICAL*1 to LOGICAL.
	Subroutine J4ARR	Changed declaration of local variable TEST from LOGICAL*1 to LOGICAL.
HLIM.FOR	Subroutine REGMOD	Removed argument HBOT from call to PARAM since it is not used by that routine. Removed last argument in call to PARAM since it is no longer used by that routine. Removed local variable HBOT since it is no longer used. Replaced call to SOLZA with call to SOLSZA.
HLISM.FOR	Subroutine HLISM	Removed local variable MFLAG since it is no longer used.
INDIRECT.INC	n/a	Removed common block INDIRECT variable ESWITCH since it is no longer used.
INIT.FOR	Subroutine LDITER	Changed declaration of output argument LAYFLG from LOGICAL*1 to LOGICAL.
	Subroutine GETFC	Changed declaration of local variable ERROR from LOGICAL*1 to LOGICAL.
	Subroutine LUDCMP	Changed PAUSE statement to STOP statement.
IO_UTIL.FOR	Subroutine UDETID	Added input argument UT. Argument DAY is no longer converted to a real number in call to SOLDEC. Added argument UT to call to SOLDEC.
LAYFLG.INC	n/a	Changed declaration of common block LAYFLG variable LAYFLG from LOGICAL*1 to LOGICAL.

Module	Program Unit	Description of Changes (continued)
LOW_PARA.FOR	Subroutine LOW_PARAM	Rewrite for optimization and readability. Removed input argument LAYR since it is no longer used. Changed intrinsic function ALOG to its generic equivalent LOG.
MATH_UTI.FOR	Subroutine INTRP	Modified logic to eliminate arithmetic IF statements.
	Subroutine SVDCMP	Changed PAUSE statement to PRINT statement.
MID_PARA.FOR	Subroutine MID_PARAM	Rewrite for optimization and readability. Removed input argument LAYR since it is no longer used. Changed intrinsic function ALOG to its generic equivalent LOG.
OUTPUT.FOR	Subroutine FINAL	Changed declaration of local variable TEST from LOGICAL*1 to LOGICAL.
PARAM.FOR	Subroutine PARAM	Rewrite for optimization and readability. Fixed a bug in the conversion of UT from hours to HHMM for the call to F2URSI. In the mid/high-latitude transition region, weighted averages of mid-latitude and high-latitude peak densities and heights are now used in the merging of profiles instead of the mid-latitude peak density and height. In the low/mid-latitude transition region, the peak density used to merge profiles is calculated from a weighted average of low-latitude and mid-latitude peak density instead of a weighted average of low-latitude and mid-latitude critical frequency, to be consistent with the profile merging process. Simplified logic since LAYR flag is no longer used. Removed input argument LAYR since it is no longer used. Removed input argument HBOT since it is not used. Removed last argument from calls to USUMODEL since it is no longer used. A single call to USUMODEL is now used instead of two calls. Removed last argument from calls to MID_PARAM since it is no longer used. A single call to MID_PARAM is now used instead of two calls. Removed last argument from calls to LOW_PARAM since it is no longer used. A single call to LOW_PARAM is now used instead of two calls. Removed call to GET_FOE since it is no longer used. Removed logic involving common block INDIRECT variable ESWITCH since it is no longer used. Changed intrinsic function ALOG to its generic equivalent LOG.
PRISM.FOR	Program PRISM	Updated the version number and version date.
READ_DBA.FOR	Subroutine READ_DBASES	Added argument UT to call to RDLOW.
	Subroutine RDLOW	Added input argument UT. Added argument UT to call to LDETID.
	Subroutine LDETID	Added input argument UT. Argument DAY is no longer converted to a real number in call to SOLDEC. Added argument UT to call to SOLDEC.
	Subroutine READ_E	Added argument UT to call to EDETID.
	Subroutine EDETID	Added input argument UT. Argument DAY is no longer converted to a real number in call to SOLDEC. Added argument UT to call to SOLDEC.
	Subroutine READMID	Added argument UT to call to DETID.
	Subroutine DETID	Added input argument UT. Argument DAY is no longer converted to a real number in call to SOLDEC. Added argument UT to call to SOLDEC.
	Subroutine READUSU	Added argument UT to calls to UDETID.
RTA.FOR	Subroutine RTA	Changed declaration of local variable IERR from LOGICAL*1 to LOGICAL.
	Subroutine CORRECTI	Rewrite for optimization and readability. If one or more data points is within the critical distance of the point of interest, then the correction at the point of interest is now calculated as the average of corrections from those data points instead of the correction of the last data point within the critical distance being used.
	Subroutine COR_MAX	Changed declaration of output argument IERR from LOGICAL*1 to LOGICAL.
	Subroutine GET_ONE_FO	Changed declaration of output argument IERR from LOGICAL*1 to LOGICAL.
	Subroutine COR_PRO	Changed declaration of output argument IERR from LOGICAL*1 to LOGICAL.
USER_INP.FOR	Subroutine CHECK_STAT	Changed declaration of input argument TEST from LOGICAL*1 to LOGICAL.
	Subroutine GIVE_DATA	Changed declaration of local variable TEST from LOGICAL*1 to LOGICAL.

Module	Program Unit	Description of Changes (continued)
USUMODEL.FOR	Subroutine USUMODEL	Rewrite for optimization and readability. Removed input argument LAYR since it is no longer used. Changed intrinsic function ALOG to its generic equivalent LOG.
	Subroutine RECON	Replaced input argument XNMLAT with input arguments SMLATE and SMLATF. Replaced argument XNMLAT with argument SMLATE and SMLATF in call to FOUR_COEFF. Removed argument LAYR from calls to FOUR_COEFF and FULL_DATA. Removed input argument LAYR since it is no longer used.
	Subroutine FOUR_COEFF	Replaced input argument XNMLAT with input arguments SMLATE and SMLATF. Fourier coefficients are now calculated for all three ions. Removed input argument LAYR since it is no longer used.
	Subroutine FULL_DATA	Altitude profiles are now calculated for all three ions. Removed input argument LAYR since it is no longer used.

The figure below illustrates the improvement in the merging of the regional parameterized models. It shows a profile of f_oF_2 vs. geographic latitude. Note the discontinuity in PRISM 1.6b f_oF_2 in the mid/high-latitude transition region and the smoother transition in the PRISM 1.7 profile. The differences at low latitudes are due to the change in the low/mid-latitude transition method and the corrected LLF parameterized model coefficients.



test.out

Year: 1996

Day: 80

UT: 12.00 hr

$F_{10.7}$: 193.0

SSN: 150.0

K_p : 3.0

Lon: 150.0 °E geographic

M·E·M·O·R·A·N·D·U·M

DATE: 7-November-1996

TO: Rob Daniell

FROM: Lincoln Brown

RE: Changes to PRISM 1.7 for PRISM 1.7a

The changes to PRISM 1.7 for PRISM 1.7a focus on improvements to the real-time data ingestion. The changes are summarized as follows:

- I. **BUG FIX:** The presence of all five possible DISS real-time data files no longer causes an array-out-of-bounds error in the DISS data ingestion. Previously, if root names for all five DISS data files were given in the PATH_NAM.TXT file, then the DISS data ingestion would attempt to access a nonexistent sixth element of the array that holds the DISS data file root names. This problem has been eliminated due to the rewrite of the DISS data ingestion (see item 5).
- II. **BUG FIX:** The presence of all five possible IMS real-time data files no longer causes an array-out-of-bounds error in the IMS data ingestion. Previously, if root names for all five IMS data files were given in the PATH_NAM.TXT file, then the IMS data ingestion would attempt to access a nonexistent sixth element of the array that holds the IMS data file root names. This problem has been eliminated due to the rewrite of the IMS data ingestion (see item 6).
- III. **BUG FIX:** The presence of all eight possible DMSP real-time data files no longer causes an array-out-of-bounds error in the DMSP data ingestion. Previously, if root names for all eight DMSP data files were given in the PATH_NAM.TXT file, then the DMSP data ingestion would attempt to access a nonexistent sixth element of the array that holds the DMSP data file root names. This problem has been eliminated due to the rewrite of the DMSP data ingestion (see item 7).
- IV. **BUG FIX:** Large amounts of DISS f_oF₂ real-time data and/or large amounts of IMS real-time data no longer cause an array-out-of-bounds error in the midlatitude correction algorithm. Previously, array allocation in the midlatitude correction algorithm for corrections for these kinds of data was inconsistent with limits defined in the real-time data ingestion. This problem was reported by David Coxwell at Air Force Institute of Technology. This problem has been eliminated due to the rewrite of the DISS and IMS data ingestion (see items 5 and 6) and the rewrite of the midlatitude correction algorithm (see item 9).
- V. The DISS real-time data ingestion has been rewritten for speed and readability. A single pass through the DISS data is now required instead of two passes. Up to 850 DISS data records can now be accepted (i.e. meet criteria for use in the real-time adjustment) from all DISS data files combined, a reduction from the previous limit of 7000 accepted

records per DISS data file. The limit of 850 accepted DISS data records is based on 50 DISS stations and a 15 minute time resolution in a [-2,2] hour time window relative to the time of the run.

- VI. The IMS data ingestion has been rewritten for speed and readability. A single pass through the IMS data is now required instead of two passes. Up to 21600 IMS data records can now be accepted (i.e. meet criteria for use in the real-time adjustment) from all IMS data files combined, a reduction from the previous limit of 7000 accepted records per IMS data file. The limit of 21600 accepted IMS data records is based on 200 IMS stations reporting 12 simultaneous measurements and a time resolution of 15 minutes in a [-2,2] hour time window relative to the time of the run.
- VII. The DMSP data ingestion has been rewritten for speed and readability. A single pass through the DMSP data is now required instead of three passes. Up to 24 sets of each of the three kinds of DMSP data are now accepted by PRISM from all DMSP data files combined, a reduction from the previous limit of 24 sets per DMSP data file. The limit of 24 sets is based on 8 satellites, an orbital period of 6060 seconds, and a [-2,2] hour time window relative to the time of the run. Up to 1451 SSIES ION DRIFT data records can be accepted (i.e. meet criteria for use in determining equatorward trough boundaries) per set, a limit which has not changed. The limit of 1451 accepted SSIES ION DRIFT data records is based on a 5 second time resolution in a [-2,0] hour time window relative to the time of the run, with 10 extra records allowed for orbital overlap. Up to 3848 SSIES IN SITU PLASMA data records can now be accepted (i.e. meet criteria for use in the real-time adjustment) from all DMSP data files combined, a reduction from the previous limit of 1451 accepted records per DMSP data file. The limit of 3848 accepted SSIES IN SITU PLASMA data records is based on 8 satellites and a time resolution of 30 seconds in a [-2,2] hour time window relative to the time of the run. Up to 7211 SSJ/4 data records can be accepted (i.e. meet criteria for use in determining auroral oval boundaries and for use in the real-time adjustment) per set, a limit which has not changed. The limit of 7211 accepted SSJ/4 data records is based on a time resolution of 1 second in a [-2,0] hour time windows relative to the time of the run, with 10 extra records allowed for orbital overlap.
- VIII. The output station list determination has been rewritten for speed and readability. A single pass through the output station list is now required instead of two passes. The number of output stations is now unlimited, a change from the previous limit of 7000 stations.
- IX. The midlatitude correction algorithm has been rewritten for the following reasons:
 - A. To optimize for speed.
 - B. To prevent extraneous zero corrections from being included in the real-time adjustment. The extraneous corrections were not based on valid data, and, although zero, influenced the correction fields and increased run time.
 - C. To remove coding for BOTTOMSIDE data since that data type is no longer considered by PRISM.
 - D. To remove redundant and commented-out coding.
 - E. To improve readability.
- X. Limits on the ingestion of real-time data are now globally defined in new INCLUDE file *rtdlimit.inc*.

XI. The HLE model has been removed since it is no longer used. All components of PRISM upon which HLE solely depends have also been removed, such as the MSIS-86 neutral atmosphere model and a number of INCLUDE files. The HLE data files CHEM.FIL, TIMING.FIL, and SOLAR.FIL are no longer used. The path to the HLE files is still read from the PATH_NAM.TXT file for compatibility, but it is not used.

XII. Coding for the BOTTOMSIDE data type has been removed since it is no longer considered in PRISM.

XIII. INCLUDE file *dlta.inc* has been removed since it is not used.

XIV. A number of unused PARAMETERS and variables have been removed.

The performance gain due to these changes is hard to predict since it depends on the amount and character of the real-time data. For many of the standard test cases provided with delivery, run-time has been decreased by about 15%. The memory requirement has been reduced by about 0.5 MB, a 7% decrease.

The table below describes the changes that I made to PRISM 1.7 to produce PRISM 1.7a.

Module	Program Unit	Description of Changes
ALPHAN.INC	n/a	Removed since it is no longer used.
CHEM.INC	n/a	Removed since it is no longer used.
DLTA.INC	n/a	Removed since it is no longer used.
ESPECT.INC	n/a	Removed since it is no longer used.
CGM_UTIL.FOR	Subroutine BNDRY	Added INCLUDE statement for INCLUDE file rtdlimit.inc.
ENVIRON.FOR	Subroutine NEUATM	Removed since it is no longer used.
	Subroutine GTSS	Removed since it is no longer used.
	Function DENSS	Removed since it is no longer used.
	Function GLOBE5	Removed since it is no longer used.
	Function GLOB5L	Removed since it is no longer used.
	Function DNET	Removed since it is no longer used.
	Function CCOR	Removed since it is no longer used.
	Block Data PRMDTD	Removed since it is no longer used.
	Function SOLANG	Removed since it is no longer used.
	Subroutine SOLSUB	Removed since it is no longer used.
	Function SOLSZA	Removed since it is no longer used.
GETDAT.FOR	Subroutine GETDAT	Replaced call to routine DO_DIR with calls to routine INRTD and routine DETOSL. Removed output parameter SUSI since it is not used. Removed PARAMETERS NSTA and MAXTYPE since they are no longer used. Removed local variable NDAT since it is no longer used.
	Subroutine DO_DIR	Removed since it is no longer used (it has been replaced by routine INRTD).
	Subroutine DO_IONO	Removed since it is no longer used (it has been replaced by routines INDISS and DETOSL).
	Subroutine DO_TEC	Removed since it is no longer used (it has been replaced by routine INIMS).
	Subroutine DO_DMSP	Removed since it is no longer used (it has been replaced by routine INDMSP).
	Subroutine INRTD	New routine.
	Subroutine INDISS	New routine.
	Subroutine INIMS	New routine.
	Subroutine INDMSP	New routine.
	Subroutine DETOSL	New routine.
	Subroutine PREC_DATA	Output parameter NREC is now initialized to zero. PRECIPITATION records are now written to data file at the current file position instead of the end of the file. A PRECIPITATION data header is no longer written to the data file. Standard deviation placeholders are no longer included in the data record written to the data file. INCLUDE statements for INCLUDE files dpath.inc and direct_d.inc have been removed since they are no longer needed. Removed local variable DUMMY since it is no longer used.
	Subroutine LOADDIR	Removed since it is no longer used.
HLEMODEL.FOR	n/a	Removed since it is no longer used.
HLIM.FOR	Subroutine REGMOD	Removed coding for HLE model since it is no longer used. Removed input parameters F10ANA, RF10NA, and APNA since they are no longer used. Removed local variables SZA, HMED, and ZNEU since they are no longer used. Removed PARAMETER NZNEU since it is no longer used. Removed coding for BOTTOMSIDE data since the BOTTOMSIDE data type is no longer used. Removed INCLUDE statement for INCLUDE file phys4_co.inc since it is not needed.
HLISM.FOR	Subroutine HLISM	Removed arguments RF10P7, F10P7A, and AP from call to routine MATRIX since they are no longer used by that routine. Removed input parameters RF10P7, F10P7A, and AP since they are no longer used.
	Subroutine MATRIX	Removed arguments F10P7A, RF10P7, and AP from calls to routine REGMOD since they are no longer used by that routine. Removed input parameters RF10P7, F10P7A, and AP since they are no longer used.
INIT.FOR	Subroutine INITPR	Added INCLUDE statement for INCLUDE file rtdlimit.inc. PARAMETER MAXORB has been renamed to MORBIT.
INT.INC	n/a	Removed since it is no longer used.
LOGICUNI.INC	n/a	Removed PARAMETERS LUIDL, LUNATM, LUNUMB, LURATE, LURI, LURO, LUSGP, and LUTEMP since they are not used. Removed PARAMETERS LUCHEM, LUSOLR, and LUTIME since they are no longer used.
LT.INC	n/a	Removed since it is no longer used.

Module	Program Unit	Description of Changes (continued)
MATH_UTI.FOR	Subroutine RTBIS	Removed since it is no longer used.
	Subroutine INTRP	Removed since it is no longer used.
	Subroutine CHMRRC	Removed since it is no longer used.
MATH4_CO.INC	n/a	Removed PARAMETERS DPH, PIO2, and TWOPI since they are not used.
MIDLAT.FOR	Subroutine MIDLAT	Rewrite for the following reasons: 1. To optimize calculation of corrections. 2. To prevent extraneous zero corrections from being included in the real-time adjustment. The extraneous corrections were not based on valid data, and although zero, did influence the correction fields, and increased run time. 3. To remove coding for BOTTOMSIDE data since that data type is no longer used. 4. To remove redundant and commented-out coding. 5. To improve readability. Removed arguments F10P7A, RF10P7, and AP from calls to routine REGMOD since they are no longer used by that routine.
	Subroutine PER_ARR	Removed since it is no longer used.
NATMOS.INC	n/a	Removed since it is no longer used.
NEUATM..INC	n/a	Removed since it is no longer used.
NEWFIT.INC	n/a	Combined common blocks INWFT and NEWFT into common block NEWFIT. Removed variables NHFM, NFFM, NHEM, NFEM, NB1M, NB1D, NB2M, NB2D, NHTM, NNTM, FFDATA, EFDATA, FHDATA, EHDATA, B1DATA, B2DATA, NTDATA, HTDATA, BT1LAT, BT1LON, BT2LAT, BT2LON, B1C, and B2C from common block NEWFIT since they are no longer used. Replaced PARAMETERS NMAX and NNMAX with PARAMETERS MFFD, MHFD, MFED, MHED, MNTD, and MHTD. The new PARAMETERS are dependent on PARAMETERS in INCLUDE file rtdlimit.inc.
OUTPUT.FOR	Subroutine GRID_OUTPUT	Removed arguments F10P7A, RF10P7, and AP from call to routine REGMOD since they are no longer used by that routine. Removed INCLUDE statement for INCLUDE file dlta.inc since it is not used.
	Subroutine STATION_OUTPUT	Removed arguments F10P7A, RF10P7, and AP from call to routine REGMOD since they are no longer used by that routine.
PHANTOM.FOR	Subroutine PHANTM	Removed arguments F10P7A, RF10P7, and AP from calls to routine REGMOD since they are no longer used by that routine. Removed INCLUDE statement for INCLUDE file indirect.inc since it is no longer needed.
PHYS4_CO.INC	n/a	Removed since it is no longer used.
PRECIP.FOR	Subroutine PRECIP	Added INCLUDE statement for INCLUDE file rtdlimit.inc.
PRECIP.INC	n/a	PARAMETER MAXORB has been moved to INCLUDE file rtdlimit.inc and renamed to MORBIT.
PRISM.FOR	Block Data PREC	Added INCLUDE statement for INCLUDE file rtdlimit.inc. PARAMETER MAXORB has been renamed to MORBIT.
	Program PRISM	Removed argument SUSI from call to routine GETDAT since it is not used. Removed arguments RF10P7, F10P7A, and AP from calls to routine HLISM since they are no longer used by that routine. Removed INCLUDE statement for INCLUDE file dlta.inc since it is not used. Updated the version number and version date.
PSPECT.INC	n/a	Removed since it is no longer used.
READ_DBA.FOR	Subroutine DBASES	Removed argument PLHE(J9:J10) from call to routine READ_DBASES since it is no longer used by that routine. Removed local variables J9 and J0 since they are no longer used.
	Subroutine READ_DBASES	Removed call to routine RDFILES since it is no longer needed. Removed input parameter HLEPATH since it is no longer used.
	Subroutine RDFILES	Removed since it is no longer used.
	Subroutine RDCHEM	Removed since it is no longer used.
	Subroutine RDTIME	Removed since it is no longer used.
	Subroutine RDSOLR	Removed since it is no longer used.

Module	Program Unit	Description of Changes (continued)
RTA.FOR	Subroutine RTA	Added INCLUDE statement for INCLUDE file rtdlimit.inc. Removed arguments FFDATA, EFDATA, FHDATA, EHDATA, NTDATA, and HTDATA from calls to routine CORRECT1 since they are no longer used by that routine. Removed arguments NMAX and NNMAX from calls to routine CORRECT1 since they are no longer used by that routine. Removed coding for BOTTOMSIDE data since the BOTTOMSIDE data type is no longer used. Removed INCLUDE statement for INCLUDE file dlta.inc since it is not used.
	Subroutine CORRECT1	Validity checking is no longer needed since all data points reaching this routine are to be used. Removed input argument MDAT since it is no longer used. Removed input argument LDAT since it is no longer used.
RTDLIMIT.INC	n/a	New file.
SOLAR.INC	n/a	Removed since it is no longer used.
SPECIE.INC	n/a	Removed since it is no longer used.
STRINGS.FOR	Subroutine STRTRM	New routine.
TIME.INC	n/a	Removed since it is no longer used.

M·E·M·O·R·A·N·D·U·M

DATE: 14-February-1997

TO: Rob Daniell

FROM: Lincoln Brown

RE: Changes to PRISM 1.7a for PRISM 1.7b

The changes to PRISM 1.7a for PRISM 1.7b focus on miscellaneous bug fixes. The changes are summarized as follows:

1. **BUG FIX:** The maximum allowed number of real-time IMS data points that PRISM can accept has been changed from 21,600 to 40,800 in order to be consistent with the I/O Specification ("200 IMS stations reporting 12 simultaneous measurements and a time resolution of 15 minutes in a +/- 2 hour time window centered on the date and UT of the run", or $200 \cdot 12 \cdot [1 + 4 \cdot 60 / 15] = 40,800$). The previous value of 21,600 was consistent with a time resolution of 30 minutes ($200 \cdot 12 \cdot [1 + 4 \cdot 60 / 30] = 21,600$).
2. **BUG FIX:** Array allocation for real-time data has been increased to allow for phantom data. Previously, the presence of the maximum allowed number of real-time data points in combination with phantom data points could cause an array-out-of-bounds error in the calculation of the low/midlatitude correction fields.
3. **BUG FIX:** In the determination of the output station list from accepted real-time DISS data, the search of the direct data file for the IONOSONDE data section has been modified to prevent a read-past-end-of-file error. In subroutine DETOSL in module GETDAT.FOR, variable NSTOUT is now reinitialized to zero after a non-IONOSONDE data section in the direct data file is skipped over during the search. Previously, if the direct data file contained one or more non-IONOSONDE data sections, but contained no IONOSONDE data section, the value of NSTOUT from the last non-IONOSONDE data section would be used to attempt to read an IONOSONDE data section past the end of the direct data file, resulting in a run-time error.
4. **BUG FIX:** In the determination of the output station list from accepted real-time DISS data, the corrected geomagnetic local times of the output stations now correspond to the day of the year and Universal Time of the run. Previously, the corrected geomagnetic local times of the DISS data records were used for the output stations, resulting in as much as a 2 hour error in corrected geomagnetic local time.

PRISM's memory requirement has been increased by about 0.25 MB, a 3% increase. Its run-time will be unaffected unless the output station list is taken from a very large set of accepted DISS data.

The table below describes the changes that I made to PRISM 1.7a to produce PRISM 1.7b.

Module	Program Unit	Description of Changes
GETDAT.FOR	Subroutine INDISS	A maximum of MDISS-MPIONO DISS data records are now accepted instead of a maximum of MDISS DISS data records in order to leave room for phantom DISS data.
	Subroutine INDMSP	A maximum of MISP-MPINSI SSIES IN SITU PLASMA data records are now accepted instead of a maximum of MISP SSIES IN SITU PLASMA data records in order to leave room for phantom SSIES IN SITU PLASMA data.
	Subroutine DETOSL	Variable NOUTST is now reinitialized to zero after non-IONOSONDE data sections in the direct data file are skipped over. When the output station list is taken from the DISS data list, the corrected geomagnetic local time of an output station list record is now calculated from the nominal day of the year and Universal Time instead of being taken from the corresponding DISS data record.
PHANTOM.FOR	Subroutine PHANTM	Moved PARAMETERS NZMLAI, NZMLAP, NZMLOI and NZMLOP to INCLUDE file rtdlimit.inc. Added INCLUDE statement for INCLUDE file rtdlimit.inc.
PRISM.FOR	Program PRISM	Updated the version number and version date.
RTDLIMIT.INC	n/a	Moved PARAMETERS NZMLAI, NZMLAP, NZMLOI, and NZMLOP from subroutine PHANTM. Added PARAMETERS MPIONO and MPINSI. Changed value of PARAMETER MDISS from 850 to 850+MPIONO. Changed value of PARAMETER MIMS from 21600 to 40800. Changed value of PARAMETER MISP from 3848 to 3848+MPINSI.

Appendix B

Derivation of the Multi-ion Ambipolar Diffusion Equation for GTIM

Robert E. Daniell, Jr. and Robert W. Simon

Computational Physics, Inc.

20 November 1996

Revised 29 August 1997

(Internal CPI Document)

The material in this Appendix was largely developed under SBIR contract F19628-96-C0041 and appeared as Appendix B of PL-TR-97-2118 ("A New, Improved Ionospheric Correction Algorithm for Single Frequency GPS Receivers").

Derivation of the Multi-ion Ambipolar Diffusion Equation for GTIM

Robert E. Daniell, Jr. and Robert W. Simon

Computational Physics, Inc.

20 November 1996

Revised 29 August 1997

0. Notation

Although we have attempted to stay close to the notation of *Anderson* [1973], we found it necessary to change the notation in some cases. Here is a summary.

Subscripts:

- α denotes charged species, ions *and* electrons
- s denotes any species, charged or neutral
- i, j denote *positive* ions
- m, n denote neutral species
- e denotes electrons

Scalar quantities

- n denotes concentration (number density) (m^{-3})
- q denotes charge (C)
- m denotes mass (kg)
- π denotes volume production rate ($\text{m}^{-3} \text{s}^{-1}$) due to photoionization or chemical reaction
- λ denotes volume loss frequency due to chemistry (s^{-1})
- ν denotes collision frequency (s^{-1})
- $\omega = qB/m$ denotes the gyrofrequency (rad s^{-1})
- T denotes temperature (K)
- α, β, γ denotes the Euler potentials
- $v = \mathbf{v} \cdot \mathbf{b}$ denotes the velocity component parallel to the magnetic field (corresponds to Dave's V_{\parallel} and U_{\parallel})
- k denotes Boltzmann's constant ($1.3807 \times 10^{-23} \text{ J K}^{-1}$)
- e denotes the magnitude of the charge on an electron ($1.6022 \times 10^{-19} \text{ C}$)

Vector quantities

- \mathbf{v} denotes velocity (m s^{-1})
- \mathbf{E} denotes electric field (V m^{-1})
- \mathbf{B} denotes magnetic induction (T)
- $\mathbf{b} = \mathbf{B}/B$ denotes a unit vector parallel to \mathbf{B} (similar to Dave's \hat{i}_{\parallel} , but opposite in sign.)
- \mathbf{g} denotes gravitational acceleration (m s^{-2})

Tensor quantities

- \mathbf{P} denotes the pressure tensor (stress tensor) ($\text{Pa} = \text{N m}^{-2}$)

1. Basic Equations

The basic equation used in ionospheric modeling is the continuity equation:

$$\frac{\partial n_\alpha}{\partial t} + \nabla \cdot (n_\alpha \mathbf{v}_\alpha) = \pi_\alpha - \lambda_\alpha n_\alpha \quad (1.1)$$

The terms on the right hand side of the equation represent the volume photochemical production (π_α) and loss (λ_α) rates. The subscript α denotes any charged species, i.e., both electrons and ions. (In this and all subsequent equations, bold serif denotes vectors and matrices, while bold sans serif denotes tensors.) In order to solve the continuity equation for $n_\alpha(\mathbf{x}, t)$, we need an expression for $\mathbf{v}_\alpha(\mathbf{x}, t)$, which we may obtain from the momentum conservation equation:

$$\frac{\partial}{\partial t} (n_\alpha m_\alpha \mathbf{v}_\alpha) + \nabla \cdot (n_\alpha m_\alpha \mathbf{v}_\alpha \mathbf{v}_\alpha) = n_\alpha m_\alpha \mathbf{g} + n_\alpha q_\alpha (\mathbf{E} + \mathbf{v}_\alpha \times \mathbf{B}) - \nabla \cdot \mathbf{P}_\alpha - \sum_s n_\alpha m_\alpha \nu_{\alpha s} (\mathbf{v}_\alpha - \mathbf{v}_s) \quad (1.2)$$

The last term on the right hand side is the rate of change of momentum carried by species α as a result of collisions with other particles, denoted by subscript s . (Note that α ranges over charged species i and e , while s ranges over both charged species and neutral species n . At this point, if considering *all* momentum sources and sinks (including photochemical processes), the proper step would be to use the continuity equation to transform the left-hand side into the substantial derivative of \mathbf{v}_α . However, for ionospheric modeling purposes, these additional terms are negligible compared to the effects of collisions, so at this point we simply neglect inertial terms. That is, we assume that the ionospheric plasma is in approximate force balance.

$$n_\alpha m_\alpha \mathbf{g} + n_\alpha q_\alpha (\mathbf{E} + \mathbf{v}_\alpha \times \mathbf{B}) - \nabla \cdot \mathbf{P}_\alpha - \sum_s n_\alpha m_\alpha \nu_{\alpha s} (\mathbf{v}_\alpha - \mathbf{v}_s) = 0 \quad (1.3)$$

which may be rearranged to produce

$$\nu_\alpha n_\alpha \mathbf{v}_\alpha - \omega_\alpha (n_\alpha \mathbf{v}_\alpha \times \hat{\mathbf{b}}) = n_\alpha \mathbf{g} + \frac{n_\alpha q_\alpha}{m_\alpha} \mathbf{E} - \frac{1}{m_\alpha} \nabla \cdot \mathbf{P}_\alpha + n_\alpha \sum_{s \neq \alpha} \nu_{\alpha s} \mathbf{v}_s \quad (1.4)$$

where $\nu_\alpha = \sum_{s \neq \alpha} \nu_{\alpha s}$, $\omega_\alpha = \frac{q_\alpha B}{m_\alpha}$ (the gyrofrequency), and $\hat{\mathbf{b}} = \mathbf{B} / B$ is a unit vector in the direction of the magnetic field. For GTIM we require only the component parallel to the magnetic field.

$$\nu_\alpha n_\alpha v_\alpha = n_\alpha \mathbf{g} \cdot \hat{\mathbf{b}} + \frac{n_\alpha q_\alpha}{m_\alpha} \mathbf{E} \cdot \hat{\mathbf{b}} - \frac{1}{m_\alpha} \nabla \cdot \mathbf{P}_\alpha \cdot \hat{\mathbf{b}} + n_\alpha \sum_{s \neq \alpha} \nu_{\alpha s} v_s \quad (1.5)$$

If we now assume that the pressure tensor \mathbf{P}_α is isotropic and represented by the ideal gas law, then $\nabla \cdot \mathbf{P}_\alpha = \nabla (n_\alpha k T_\alpha)$. From this we may derive the usual expression for the flux in terms of a diffusion coefficient and the density gradient.

$$n_\alpha v_\alpha = \frac{1}{v_i} \left[-\frac{k}{m_\alpha} \nabla(n_\alpha T_\alpha) \cdot \mathbf{b} + n_\alpha \mathbf{g} \cdot \mathbf{b} + \frac{n_\alpha q_\alpha}{m_\alpha} \mathbf{E} \cdot \mathbf{b} + n_\alpha \sum_\beta v_{\alpha\beta} v_\beta \right] \quad (1.6)$$

Note that because we have stopped with the momentum equation and neglected the energy and heat flow equations, we do not obtain the “thermal diffusion” terms of *St.-Maurice and Schunk* [1976], which also appear in *Schunk and Nagy* [1980] and *Young et al.* [1980a, 1980b].

2. General Equations for Multi-species Ionospheric Diffusion and Chemistry

If the scale length of the plasma is much greater than a Debye Length, then charge imbalances will not persist much longer than $\tau_p = \frac{2\pi}{\omega_p}$. This means that as long as we do not wish to model plasma waves, we may impose both the charge neutrality condition

$$n_e = \sum_i n_i \quad (2.1)$$

and the flux balance condition

$$n_e v_e = \sum_i n_i v_i \quad (2.2)$$

where e denotes electrons and i denotes ions. The flux balance condition is the necessary condition for ambipolar diffusion, and allows us to eliminate \mathbf{E} from the force balance equations by writing the electron equation as

$$\mathbf{E} \cdot \mathbf{b} = -\frac{1}{e} \left[\frac{m_e}{n_e} v_e (n_e v_e) + \frac{k}{n_e} \nabla(n_e T_e) \cdot \mathbf{b} - m_e \mathbf{g} \cdot \mathbf{b} - m_e \sum_{\beta \neq e} v_{e\beta} v_\beta \right] \quad (2.3)$$

This result may be substituted into the equation for ion species i to yield

$$n_i v_i = \frac{1}{v_i} \left\{ -\frac{k}{m_i} \mathbf{b} \cdot \nabla(n_i T_i) + n_i \mathbf{g} \cdot \mathbf{b} + n_i \sum_s v_{is} v_s - \frac{n_i q_i}{m_i e} \left[\frac{m_e}{n_e} v_e \left(\sum_j n_j v_j \right) + \frac{k}{n_e} \mathbf{b} \cdot \nabla(n_e T_e) - m_e \mathbf{g} \cdot \mathbf{b} - m_e \sum_{s \neq e} v_{es} v_s \right] \right\}$$

where j , like i , denotes only positive ions. Rearranging and collecting terms results in

$$n_i v_i = \frac{1}{v_i} \left\{ -\frac{k}{m_i} \left[\mathbf{b} \cdot \nabla(n_i T_i) + \frac{n_i q_i}{n_e e} \mathbf{b} \cdot \nabla(n_e T_e) \right] + n_i \left[1 + \frac{m_e q_i}{m_i e} \right] \mathbf{g} \cdot \mathbf{b} \right\} \\ + \frac{1}{v_i} \left\{ n_i \sum_s \left[v_{is} + \frac{m_e q_i}{m_i e} v_{es} \right] v_s - \frac{m_e q_i n_i}{m_i e n_e} \left(v_e \sum_j n_j v_j \right) \right\} \quad (2.4)$$

where the sum over j is over all ion species. To simplify the summation, we assume $v_{ii} = v_{ee} = 0$. The above expression may be simplified somewhat if we assume that all ion species i (or j) are singly charged positive ions so that $q_i = e$:

$$n_i v_i = \frac{1}{v_i} \left\{ -\frac{k}{m_i} \left[\mathbf{b} \cdot \nabla(n_i T_i) + \frac{n_i}{n_e} \mathbf{b} \cdot \nabla(n_e T_e) \right] + n_i \left[1 + \frac{m_e}{m_i} \right] \mathbf{g} \cdot \mathbf{b} \right\} \\ + \frac{1}{v_i} \left\{ n_i \sum_s \left[v_{is} + \frac{m_e}{m_i} v_{es} \right] v_s - \frac{m_e n_i}{m_i n_e} \left(v_e \cdot \sum_j n_j v_j \right) \right\} \quad (2.5)$$

To produce a useful expression, we must collect all terms involving the flux of the i^{th} species on the left hand side of the equation. To do so, however, we must first examine the collision terms:

$$n_i \sum_s \left(v_{is} + \frac{m_e}{m_i} v_{es} \right) v_s = n_i \frac{m_e}{m_i} v_{ei} v_i + n_i v_{ie} v_e + n_i \sum_{s \neq e, i} \left(v_{is} + \frac{m_e}{m_i} v_{es} \right) v_s \quad (2.6)$$

The first term may be rewritten

$$n_i \frac{m_e}{m_i} v_{ei} v_i = \frac{n_i}{n_e} v_{ie} n_i v_i$$

where we have used the relation $n_i m_i v_{ie} = n_e m_e v_{ei}$ [Schunk and Nagy, 1980]. Similarly, the second term may be rewritten

$$n_i v_{ie} v_e = \frac{n_i}{n_e} v_{ie} n_e v_e = \frac{n_i}{n_e} v_{ie} \sum_j n_j v_j \quad (2.7)$$

or

$$n_i v_{ie} v_e = \frac{n_i}{n_e} v_{ie} n_i v_i + \frac{n_i}{n_e} v_{ie} \sum_{j \neq i} n_j v_j$$

Thus, Eq. (2.6) may be rewritten as

$$n_i \sum_s \left(v_{is} + \frac{m_e}{m_i} v_{es} \right) v_s = 2 \frac{n_i}{n_e} v_{ie} n_i v_i + \frac{n_i}{n_e} v_{ie} \sum_{j \neq i} n_j v_j + n_i \sum_{s \neq e, i} \left(v_{is} + \frac{m_e}{m_i} v_{es} \right) v_s \quad (2.8)$$

This is to be combined with the other collision term so that

$$n_i \sum_s \left[v_{is} + \frac{m_e}{m_i} v_{es} \right] v_s - \frac{m_e}{m_i} \frac{n_i}{n_e} \left(v_e \sum_j n_j v_j \right) = 2 \frac{n_i}{n_e} v_{ie} n_i v_i - \frac{m_e}{m_i} \frac{n_i}{n_e} v_e (n_i v_i) \\ + \frac{n_i}{n_e} v_{ie} \sum_{j \neq i} n_j v_j + n_i \sum_{s \neq e, i} \left(v_{is} + \frac{m_e}{m_i} v_{es} \right) v_s - \frac{m_e}{m_i} \frac{n_i}{n_e} \left(v_e \sum_{j \neq i} n_j v_j \right)$$

which may be rewritten

$$n_i \sum_s \left[v_{is} + \frac{m_e}{m_i} v_{es} \right] v_s - \frac{m_e}{m_i} \frac{n_i}{n_e} \left(v_e \sum_j n_j v_j \right) = \frac{n_i}{n_e} \left(2 v_{ie} - \frac{m_e}{m_i} v_e \right) n_i v_i \\ + \frac{n_i}{n_e} \left(v_{ie} - \frac{m_e}{m_i} v_e \right) \cdot \sum_{j \neq i} n_j v_j + n_i \sum_{s \neq e, i} \left(v_{is} + \frac{m_e}{m_i} v_{es} \right) v_s$$

Using the above expression, we may rewrite Eq. (2.5) as

$$\left[1 + \frac{n_i}{n_e} \left(\frac{m_e}{m_i} \frac{v_e}{v_i} - 2 \frac{v_{ie}}{v_i} \right) \right] n_i v_i = \frac{1}{v_i} \left\{ - \frac{k}{m_i} \left[\mathbf{b} \cdot \nabla (n_i T_i) + \frac{n_i}{n_e} \mathbf{b} \cdot \nabla (n_e T_e) \right] \right\} \\ + \frac{1}{v_i} \left\{ n_i \left[1 + \frac{m_e}{m_i} \right] \mathbf{g} \cdot \mathbf{b} + n_i \sum_{s \neq e, i} \left(v_{is} + \frac{m_e}{m_i} v_{es} \right) v_s + \frac{n_i}{n_e} \left(v_{ie} - \frac{m_e}{m_i} v_e \right) \sum_{j \neq i} n_j v_j \right\} \quad (2.9)$$

Define

$$v_i^{eff} = v_i + \frac{n_i}{n_e} \left(\frac{m_e}{m_i} v_e - 2 v_{ie} \right) \quad (2.10)$$

$$v_i^{eff} = \sum_n \left[v_{in} + \frac{n_i}{n_e} \frac{m_e}{m_i} v_{en} \right] + \sum_{j \neq i} \left[v_{ij} + \frac{n_i}{n_e} \frac{m_e}{m_i} v_{ej} \right] + \left(1 - 2 \frac{n_i}{n_e} \right) v_{ie} + \frac{n_i}{n_e} \frac{m_e}{m_i} v_{ei} \\ v_i^{eff} = \sum_n \left[v_{in} + \frac{n_i}{n_e} \frac{m_e}{m_i} v_{en} \right] + \sum_{j \neq i} \left[v_{ij} + \frac{n_i}{n_e} \frac{m_e}{m_i} v_{ej} \right] + \left(1 - \frac{n_i}{n_e} \right)^2 v_{ie} \quad (2.11)$$

where we have once more made use of the relation $n_i m_i v_{ie} = n_e m_e v_{ei}$. Noting that corresponding electron and ion collision frequencies are not very different in magnitude, and neglecting m_e/m_i compared to terms of order unity, we may approximate

$$\nu_i^{eff} \approx \sum_n \nu_{in} + \sum_{j \neq i} \nu_{ij} + \left(1 - \frac{n_i}{n_e}\right)^2 \nu_{ie} \quad (2.12)$$

Note that for a single ion species the ion-electron collision term vanishes exactly. In the absence of a background gas of neutrals, $\nu_i^{eff} \rightarrow 0$ and the concept of ambipolar diffusion becomes invalid. This may be a concern at high altitudes where neutral densities are very low and H^+ is the dominant ion.

With the definition of ν_i^{eff} the expression for the ion flux becomes

$$\begin{aligned} n_i \nu_i = \frac{1}{\nu_i^{eff}} & \left\{ -\frac{k}{m_i} \left[\mathbf{b} \cdot \nabla (n_i T_i) + \frac{n_i}{n_e} \mathbf{b} \cdot \nabla (n_e T_e) \right] + n_i \left[1 + \frac{m_e}{m_i} \right] \mathbf{g} \cdot \mathbf{b} \right. \\ & \left. + n_i \sum_{s \neq e, i} \left(\nu_{is} + \frac{m_e}{m_i} \nu_{es} \right) \nu_s + \frac{n_i}{n_e} \left(\nu_{ie} - \frac{m_e}{m_i} \nu_e \right) \sum_{j \neq i} n_j \nu_j \right\} \end{aligned} \quad (2.13)$$

Neglecting m_e/m_i with respect to terms of order unity, the equation simplifies to

$$\begin{aligned} n_i \nu_i = \frac{1}{\nu_i^{eff}} & \left\{ -\frac{k}{m_i} \left[\mathbf{b} \cdot \nabla (n_i T_i) + \frac{n_i}{n_e} \mathbf{b} \cdot \nabla (n_e T_e) \right] + n_i \mathbf{g} \cdot \mathbf{b} \right. \\ & \left. + n_i \sum_n \nu_{in} \nu_n + n_i \sum_{j \neq i} \nu_{ij} \nu_j + n_i \left(\nu_{ie} - \frac{m_e}{m_i} \nu_e \right) \sum_{j \neq i} \frac{n_j}{n_e} \nu_j \right\} \end{aligned}$$

(The relative magnitudes of ν_{ie} and $\nu_e = \sum_n \nu_{en} + \sum_j \nu_{ej}$ is not immediately apparent, so both terms are retained.)

Now we express the pressure gradient terms in terms of the coordinates Q and X of Anderson [1973]. First, we write the explicit definition of \mathbf{b} :

$$\mathbf{b} = \frac{1}{B} (B_r \hat{\mathbf{r}} + B_\theta \hat{\boldsymbol{\theta}} + B_\phi \hat{\boldsymbol{\phi}}) = -\sin I \hat{\mathbf{r}} - \cos I \cos \delta \hat{\boldsymbol{\theta}} - \cos I \sin \delta \hat{\boldsymbol{\phi}}$$

with $B = |\mathbf{B}|$ and the standard definitions

$$\begin{aligned} \sin I & \equiv -\frac{B_r}{B} \\ \sin \delta & = -\frac{B_\phi}{\sqrt{B_\theta^2 + B_\phi^2}} \end{aligned}$$

Note that the definition of \hat{i}_l in *Anderson* [1973] has the opposite sign so that $\hat{i}_l \cdot \mathbf{B} < 0$. With our definition, $\mathbf{g} \cdot \mathbf{b} = -\mathbf{g}\hat{\mathbf{r}} \cdot \mathbf{b} = g \sin I$ where $g = |\mathbf{g}|$.

With the above definitions, the parallel component of the gradient operator is

$$\mathbf{b} \cdot \nabla = -\sin I \frac{\partial}{\partial r} - \frac{\cos I \cos \delta}{r} \frac{\partial}{\partial \theta} - \frac{\cos I \sin \delta}{r \sin \theta} \frac{\partial}{\partial \phi}$$

Define $Q \equiv \gamma / (r_0 g_l^0)$ where γ is the scalar potential such that $\mathbf{B} = -\nabla \gamma$. Then

$$\mathbf{b} \cdot \nabla = -C \frac{\partial X}{\partial Q} \frac{\partial}{\partial X}$$

where C is

$$C = \sin I \frac{\partial Q}{\partial r} + \frac{\cos I \cos \delta}{r} \frac{\partial Q}{\partial \theta} + \frac{\cos I \sin \delta}{r \sin \theta} \frac{\partial Q}{\partial \phi}$$

and X is defined as

$$X = \frac{\sinh(\Gamma Q)}{\sinh(\Gamma Q_{\max})}$$

where Q_{\max} is the value of Q at the first (northernmost) point on the field line.

For GTIM, we assume a dipole field and work in dipole coordinates (that is, in a coordinate system aligned with the dipole axis). In that case

$$\gamma(r, \theta, \phi) = g_l^0 r_0 \left(\frac{r_0}{r} \right)^2 \cos \theta$$

$$Q(r, \theta, \phi) = \left(\frac{r_0}{r} \right)^2 \cos \theta$$

$$B_r = -2g_l^0 \left(\frac{r_0}{r} \right)^3 \cos \theta, B_\theta = g_l^0 \left(\frac{r_0}{r} \right)^3 \sin \theta, B_\phi = 0, \text{ and } B = g_l^0 \left(\frac{r_0}{r} \right)^3 \sqrt{1 + 3 \cos^2 \theta}$$

so that

$$\sin I = \frac{2 \cos \theta}{\sqrt{1 + 3 \cos^2 \theta}} \text{ and } \sin \delta = 0$$

and

$$C = -\frac{r_0^2}{r^3} \sqrt{1 + 3 \cos^2 \theta}$$

In any case, we obtain the following expression for the ion flux:

$$n_i v_i = \frac{n_i g \sin I}{v_i^{eff}} + \frac{n_i}{v_i^{eff}} \sum_n v_{in} v_n + \frac{n_i}{v_i^{eff}} \sum_{j \neq i} v_{ij} v_j + \frac{n_i}{v_i^{eff}} \left(v_{ie} - \frac{m_e}{m_i} v_e \right) \sum_{j \neq i} \frac{n_j}{n_e} v_j + \frac{k}{m_i} \frac{1}{v_i^{eff}} C \frac{\partial X}{\partial Q} \left[\frac{\partial}{\partial X} (n_i T_i) + \frac{n_i}{n_e} \frac{\partial}{\partial X} (n_e T_e) \right] \quad (2.14)$$

Since v_i^{eff} contains the ratio n_i/n_e , every term in Eq. (2.14) is non-linear except in the special case of a single ion ($n_i \equiv n_e$). We argue that non-linear effects produced by v_i^{eff} are small. If $n_i \gg n_{j \neq i}$ the last term of Eq. (2.12) is negligible and

$$v_i^{eff} \approx \sum_n v_{in} + \sum_{j \neq i} v_{ij}, \quad (n_i \gg n_{j \neq i})$$

On the other hand, if $n_i \sim n_j$, write

$$\begin{aligned} v_i^{eff} &\approx \sum_n v_{in} + \sum_{j \neq i} \frac{n_j m_j}{n_i m_i} v_{ji} + \left(1 - \frac{n_i}{n_e} \right)^2 \frac{n_e m_e}{n_i m_i} v_{ei} \\ &\sim \sum_n v_{in} + \sum_{j \neq i} v_{ji} + \left(1 - \frac{n_i}{n_e} \right) \frac{m_e}{m_i} v_{ei} \end{aligned}$$

using $n_i \sim n_j \sim n_e$ and $m_j \sim m_i$. But $v_{ei} \sim v_{ji}$ and $\frac{m_e}{m_i} \ll 1$, so the last term is again negligible. Finally, if $n_i \ll n_j$ for some j , then

$$\begin{aligned} v_i^{eff} &\approx \sum_n v_{in} + \sum_{j \neq i} v_{ij} + \left(1 - \frac{n_i}{n_e} \right)^2 v_{ie} \\ &\sim \sum_n v_{in} + \sum_{j \neq i} v_{ji} + v_{ie} \end{aligned}$$

and the dependence on n_i/n_e disappears. Thus, in all cases, n_i/n_e has only a small effect and can simply be treated as a constant during each time step.

Now consider the pressure gradient terms:

$$PG \equiv \frac{k}{m_i v_i^{eff}} C \frac{\partial X}{\partial Q} \left[\frac{\partial}{\partial x} (n_i T_i) + \frac{n_i}{n_e} \frac{\partial}{\partial x} (n_e T_e) + \frac{n_i}{n_e} \sum_{j \neq i} \frac{\partial}{\partial x} (n_j T_e) \right] \quad (2.15)$$

Define

$$B_3^{(i)} \equiv -\frac{k}{m_i v_i^{\text{eff}}} C \frac{\partial X}{\partial Q} \quad (2.16)$$

so that

$$PG \equiv -B_3^{(i)} \left[\frac{\partial}{\partial x} (n_i T_i) + \frac{n_i}{n_e} \frac{\partial}{\partial x} (n_i T_e) + \frac{n_i}{n_e} \sum_{j \neq i} \frac{\partial}{\partial x} (n_j T_e) \right] \quad (2.17)$$

To cast this in a form similar to that used in LOWLAT and GTIM, write Eq. (2.17) as

$$PG \equiv -B_3^{(i)} \left\{ \frac{\partial}{\partial x} \left[\left(T_i + \frac{n_i}{n_e} T_e \right) n_i \right] + \frac{n_i}{n_e} \sum_{j \neq i} \frac{\partial}{\partial x} (n_j T_e) - n_i T_e \frac{\partial}{\partial x} \left(\frac{n_i}{n_e} \right) \right\} \quad (2.18)$$

In order to use the LOWLAT/GTIM solver, we need to write the pressure gradient terms as

$$PG \equiv -B_3^{(i)} \left[\frac{\partial}{\partial x} (T_i^{\text{eff}} n_i) + (F - G) n_i \right] \quad (2.19)$$

where $T_i^{\text{eff}} \equiv T_i + \frac{n_i}{n_e} T_e$, $F \equiv \frac{1}{n_e} \sum_{j \neq i} \frac{\partial}{\partial x} (n_j T_e)$, and $G \equiv T_e \frac{\partial}{\partial x} \left(\frac{n_i}{n_e} \right)$. We will take T_i^{eff} , F , and G as constant during a time step. Let us examine the validity of this approach.

Case 1: $n_i \gg n_{j \neq i}$

In this case $n_i/n_e \sim 1$ so holding T_i^{eff} and G constant is reasonable, while F is small.

Case 2: $n_i \ll n_e$

In this case, $T_i^{\text{eff}} \approx T_i$, and G is very small. In F , $n_e \approx n_j$ for some $j \neq i$ so neglecting its variation during the time step is also reasonable.

Case 3: $n_i \approx n_j$ (for some j)

In this case, the approximation is not valid, but we can hope that it only effects a few grid points in the transition from one dominant ion to another (e.g., from O+ dominant to H+ dominant).

Now, we rewrite the ion flux as

$$n_i v_i = B_5^{(i)} n_i - B_3^{(i)} \frac{\partial}{\partial X} (T_i^{\text{eff}} n_i) \quad (2.20)$$

where

$$B_5^{(i)} = \frac{g \sin I}{v_i^{\text{eff}}} + \frac{1}{v_i^{\text{eff}}} \sum_n v_{in} v_n + \frac{1}{v_i^{\text{eff}}} \sum_{j \neq i} v_{ij} v_j + \frac{1}{v_i^{\text{eff}}} \left(v_{ie} - \frac{m_e}{m_i} v_e \right) \sum_{j \neq i} \frac{n_j}{n_e} v_j \\ - B_3^{(i)} \left[\frac{1}{n_e} \frac{\partial}{\partial X} [(n_e - n_i) T_e] - T_e \frac{\partial}{\partial X} \left(\frac{n_i}{n_e} \right) \right]$$

Now, we need to take the divergence of this flux.

$$\nabla \cdot (n_i v_i \mathbf{b}) = \mathbf{b} \cdot \nabla (n_i v_i) + n_i v_i \nabla \cdot \mathbf{b} \quad (2.21)$$

or

$$\nabla \cdot (n_i v_i \mathbf{b}) = -C \frac{\partial X}{\partial Q} \frac{\partial}{\partial X} (n_i v_i) + n_i v_i \nabla \cdot \mathbf{b} \quad (2.22)$$

The full continuity equation becomes

$$\frac{\partial n_i}{\partial t} = \pi_i - \lambda_i n_i + C \frac{\partial X}{\partial Q} \frac{\partial}{\partial X} (n_i v_i) - n_i v_i \nabla \cdot \mathbf{b} - n_i \nabla \cdot \mathbf{V}_\perp \quad (2.23)$$

where \mathbf{V}_\perp is $(\mathbf{E} \times \mathbf{B})/B^2$. Substituting from Eq. (2.20)

$$\frac{\partial n_i}{\partial t} = \pi_i + [-\lambda_i - v_i \nabla \cdot \mathbf{b} - \nabla \cdot \mathbf{V}_\perp] n_i + C \frac{\partial X}{\partial Q} \frac{\partial}{\partial X} \left[B_5^{(i)} n_i - B_3^{(i)} \frac{\partial}{\partial X} (T_i^{\text{eff}} n_i) \right] \quad (2.24)$$

or

$$\frac{\partial n_i}{\partial t} = \pi_i - [\lambda_i + \nabla \cdot \mathbf{V}_\perp] n_i + C \frac{\partial X}{\partial Q} \frac{\partial}{\partial X} (B_5^{(i)} n_i) - C \frac{\partial X}{\partial Q} \frac{\partial}{\partial X} \left[B_3^{(i)} \frac{\partial}{\partial X} (T_i^{\text{eff}} n_i) \right] \\ - \left[B_5^{(i)} n_i - B_3^{(i)} \frac{\partial}{\partial X} (T_i^{\text{eff}} n_i) \right] \nabla \cdot \mathbf{b}$$

Keeping in mind that $Y=1$ and $G_i = n_i$, we can make the following identifications. First we write the multi-ion diffusion equation in the notation of *Anderson* [1973]:

$$\frac{\partial}{\partial t} (n_i) = B_2 \frac{\partial}{\partial X} \left[B_3^{(i)} \frac{\partial}{\partial X} (B_4^{(i)} n_i) \right] - B_2 \frac{\partial}{\partial X} (B_5^{(i)} n_i) \\ + B_6 \frac{\partial}{\partial X} (B_4^{(i)} n_i) + B_7 \frac{\partial}{\partial X} (n_i) + B_8^{(i)} n_i + B_9 \quad (2.25)$$

Then, we identify the coefficients $B_k^{(i)}$:

$$B_1 = 1; \quad B_2 = -C \frac{\partial X}{\partial Q}; \quad B_3^{(i)} = \frac{k}{m_i v_i^{eff}} B_2^{(i)}; \quad B_4^{(i)} = T_i^{eff};$$

$$B_5^{(i)} = -\frac{g \sin I}{v_i^{eff}} + \frac{\sum v_{in}}{v_i^{eff}} U_{\parallel} + \frac{1}{v_i^{eff}} \sum_{j \neq i} v_{ij}^{eff} v_j - B_3 \left\{ \frac{1}{n_e} \frac{\partial}{\partial X} [(n_e - n_i) T_e] - T_e \frac{\partial}{\partial X} \left(\frac{n_i}{n_e} \right) \right\};$$

$$B_6^{(i)} = B_3^{(i)} \nabla \cdot \mathbf{b}; \quad B_7 = -\frac{dX}{dt} \Big|_Q; \quad B_8^{(i)} = -[\lambda_i + \nabla \cdot \mathbf{V}_{\perp} + B_5 \nabla \cdot \mathbf{b}]; \quad B_9^{(i)} = \pi_i;$$

$$\text{with } v_{ij}^{eff} \equiv v_{ij} + \frac{n_j}{n_e} \left(v_{ie} - \frac{m_e}{m_i} v_e \right), \quad v_e = \sum_n v_{en} + \sum_j v_{ej}, \quad U_{\parallel} = \mathbf{U} \cdot \mathbf{b} = v_n \quad \text{and}$$

$C = \sin I \frac{\partial Q}{\partial r} + \frac{\cos I \cos \delta}{r} \frac{\partial Q}{\partial \theta} + \frac{\cos I \sin \delta}{r \sin \theta} \frac{\partial Q}{\partial \phi}$. We have assumed that all neutral species move together with a common bulk velocity.

Neutral wind models give the wind velocity components in geographic coordinates rather than geomagnetic dipole coordinates. The conversion between the two coordinate systems is not described in this document.

To avoid ambiguity, we also note that the diffusion equation as used in LOWLAT and GTIM is written in a slightly different form. The correspondence between B_k as used above and the "COEFk" that appear in the code itself is

$$\begin{array}{llll} \text{COEF1} = B_1 & \text{COEF2} = B_2 & \text{COEF3} = B_3^{(i)} & \text{COEF4} = B_4^{(i)} \\ \text{COEF5} = B_5^{(i)} & \boxed{\text{COEF6} = B_7} & \boxed{\text{COEF7} = -B_6^{(i)}} & \text{COEF8} = B_8^{(i)} \\ \text{COEF9} = B_9^{(i)} & & & \end{array}$$

3. Collision terms.

Schunk and Nagy [1980] provide expressions for the collision terms required in GTIM. We have adopted these expressions except of the resonant charge exchange between O and O⁺. For this process we have adopted the formula of *Pesnell et al.* [1993].

In the following expressions concentrations (n) are in m⁻³, temperatures are in K, masses are in kg, and collision frequencies are in s⁻¹.

$$T_{st} = \frac{m_t T_s + m_s T_t}{m_s + m_t}$$

a. collisions between O⁺ and other species

$$\nu_{O^+,N_2} = 6.82 \times 10^{-16} n_{N_2}$$

$$\nu_{O^+,O_2} = 6.64 \times 10^{-16} n_{O_2}$$

$$\begin{aligned} \nu_{O^+,O} &= 3.0 \times 10^{-17} \left[1 - 0.135 \log_{10} (10^{-3} T_{O^+,O}) \right] \sqrt{T_{O^+,O}} n_O \\ &= 5.92 \times 10^{-17} \left[1 - 0.0961 \log_{10} T_{O^+,O} \right]^2 \sqrt{T_{O^+,O}} n_O \end{aligned}$$

$$\nu_{O^+,He} = 1.32 \times 10^{-16} n_{He}$$

$$\nu_{O^+,H} = 7.44 \times 10^{-17} \left[1 - 0.047 \log_{10} T_{O^+,H} \right]^2 \sqrt{T_{O^+,H}} n_H$$

$$\nu_{O^+,He^+} = 1.4 \times 10^{-7} \frac{n_{He}}{T_{O^+,He^+}^{3/2}}$$

$$\nu_{O^+,H^+} = 7.7 \times 10^{-8} \frac{n_H}{T_{O^+,H^+}^{3/2}}$$

$$\nu_{O^+,e} = 1.85 \times 10^{-9} \frac{n_e}{T_{O^+,e}^{3/2}}$$

b. collisions between He^+ and other species

$$\nu_{He^+,N_2} = 1.60 \times 10^{-15} n_{N_2}$$

$$\nu_{He^+,O_2} = 1.53 \times 10^{-15} n_{O_2}$$

$$\nu_{He^+,O} = 1.01 \times 10^{-15} n_O$$

$$\nu_{He^+,He} = 8.73 \times 10^{-17} \left[1 - 0.093 \log_{10} T_{He^+,He} \right]^2 \sqrt{T_{He^+,He}} n_{He}$$

$$\nu_{He^+,H} = 4.71 \times 10^{-16} n_H$$

$$\nu_{He^+,O^+} = 5.7 \times 10^{-7} \frac{n_{O^+}}{T_{He^+,O^+}^{3/2}}$$

$$\nu_{\text{He}^+, \text{H}^+} = 2.8 \times 10^{-7} \frac{n_{\text{H}^+}}{T_{\text{He}^+, \text{H}^+}^{3/2}}$$

$$\nu_{\text{He}^+, e} = 7.42 \times 10^{-9} \frac{n_e}{T_{\text{He}^+, e}^{3/2}}$$

c. collisions between H^+ and other species

$$\nu_{\text{H}^+, \text{N}_2} = 3.36 \times 10^{-15} n_{\text{N}_2}$$

$$\nu_{\text{H}^+, \text{O}_2} = 3.20 \times 10^{-15} n_{\text{O}_2}$$

$$\nu_{\text{H}^+, \text{O}} = 6.61 \times 10^{-17} \left[1 - 0.047 \log_{10} T_{\text{H}^+, \text{O}} \right]^2 \sqrt{T_{\text{H}^+, \text{O}}} n_{\text{O}}$$

$$\nu_{\text{H}^+, \text{H}} = 2.65 \times 10^{-16} \left[1 - 0.083 \log_{10} T_{\text{H}^+, \text{H}} \right]^2 \sqrt{T_{\text{H}^+, \text{H}}} n_{\text{H}}$$

$$\nu_{\text{H}^+, \text{O}^+} = 1.23 \times 10^{-6} \frac{n_{\text{O}^+}}{T_{\text{H}^+, \text{O}^+}^{3/2}}$$

$$\nu_{\text{H}^+, \text{He}^+} = 1.14 \times 10^{-6} \frac{n_{\text{H}^+}}{T_{\text{H}^+, \text{He}^+}^{3/2}}$$

$$\nu_{\text{H}^+, e} = 2.97 \times 10^{-8} \frac{n_e}{T_{\text{H}^+, e}^{3/2}}$$

c. collisions between electrons and other species

$$\nu_{e, \text{N}_2} = 2.33 \times 10^{-17} (1 - 1.21 \times 10^{-4} T_{e, \text{N}_2}) \sqrt{T_{e, \text{N}_2}} n_{\text{N}_2}$$

$$\nu_{e, \text{O}_2} = 1.82 \times 10^{-16} (1 + 0.036 \sqrt{T_{e, \text{O}_2}}) \sqrt{T_{e, \text{O}_2}} n_{\text{O}_2}$$

$$\nu_{e, \text{O}} = 8.9 \times 10^{-17} (1 + 5.7 \times 10^{-4} T_{e, \text{O}}) \sqrt{T_{e, \text{O}}} n_{\text{O}}$$

$$\nu_{e, \text{H}} = 4.5 \times 10^{-17} (1 - 1.35 \times 10^{-4} T_{e, \text{H}}) \sqrt{T_{e, \text{H}}} n_{\text{H}}$$

$$\nu_{e, \text{O}^+} = 5.45 \times 10^{-5} \frac{n_{\text{O}^+}}{T_{e, \text{O}^+}^{3/2}}$$

$$\nu_{e,\text{He}^+} = 5.45 \times 10^{-5} \frac{n_{\text{He}^+}}{T_{e,\text{He}^+}^{3/2}}$$

$$\nu_{e,\text{H}^+} = 5.45 \times 10^{-5} \frac{n_{\text{H}^+}}{T_{e,\text{H}^+}^{3/2}}$$

References for Appendix B

- Anderson, D. N., A theoretical study of the ionospheric F region equatorial anomaly—I. Theory, *Planet. Space Sci.*, 21, 409-419, 1973.
- Pesnell, W. D., K. Omidvar, and W. R. Hoegy, Momentum transfer collision frequency of O^+-O , *Geophys. Res. Lett.*, 20, 1343-1346, 1993.
- Schunk, R. W., and A. F. Nagy, Ionospheres of terrestrial planets, *Rev. Geophys.*, 18, 813-852, 1980.
- St.-Maurice, J.-P., and R. W. Schunk, Diffusion and heat flow equations for the mid-latitude topside ionosphere, *Planet. Space Sci.*, 25, 907-920, 1977.
- Young, E. R., P. G. Richards, and D. G. Torr, A flux preserving method of coupling first and second order equations to simulate the flow of plasma between the protonosphere and the ionosphere, *J. Comput. Phys.*, 38, 141-156, 1980a.
- Young, E. R., D. G. Torr, P. Richards, and A. F. Nagy, A computer simulation of the midlatitude plasmasphere and ionosphere, *Planet. Space Sci.*, 28, 881-893, 1980b.